2018 European Control Conference (ECC)
June 12-15, 2018. Limassol, Cyprus

On-line fuel-efficiency optimization of Diesel engines using constrained multivariable extremum-seeking

Robert van der Weijst, Thijs van Keulen, Frank Willems

Abstract— **Advanced control concepts are required to maximize the fuel-efficiency of Diesel engines and to comply with emission legislation. The aim of this paper is to develop a controller that fully utilizes the fuel-path and air-path hardware, and is adaptive for real-world disturbances. The control design comprises a feedback control system, which uses air-path actuators and fuel injection settings to robustly track engine-out NO_x emission and engine power demands, as well as two parameters that are known to influence the NO_x emission versus fuel consumption trade-off; combustion phasing and pumping losses. Furthermore, an on-line implementable convex cost criterion is proposed that evaluates the injector opening time to obtain a cost output which is equivalent to fuel efficiency. A multivariable constrained extremum-seeking method is applied to minimize the cost output, as a function of combustion phasing and pumping losses, subject to constraints on the tracking performance of the low-level control system. The control design is implemented on a Euro-VI Diesel engine equipped with exhaust gas recirculation and a variable geometry turbine, as well as in-cylinder pressure sensors. The experiments demonstrate the effectiveness of the applied extremum-seeking approach in finding the (constrained) optimum, for a constant engine speed and torque.**

I. Introduction

Diesel engine powertrains are subject to constrained emission of pollutants, set by legislation, while at the same time, a low fuel consumption is desirable. Emission constraints are not limited to laboratory test cycles, but require real-world evaluation as well. This means the control system needs to be robust for real-world disturbances like varying ambient air conditions, varying fuel composition, production tolerances, component fouling, and wearing. As such, control of Diesel powertrains is challenging.

A typical Diesel engine powertrain consists of the engine itself and the exhaust after-treatment system (EAS). The EAS is used to reduce the engine-out emission level of the pollutants to the tailpipe-out level prescribed by legislation. However, reducing emission of the pollutant NO_x (a mixture of NO and NO_2) in the EAS, requires the addition of urea in the selective catalytic reduction (SCR) system, which is one of the components of the EAS. This increases the operational cost of the powertrain. Therefore, a relevant engine control problem, and the problem considered in this paper, is to deliver the requested power, using minimal fuel, while satisfying an engine-out NO_x constraint. Available mechanisms to suppress engine-out NO_x emission are exhaust gas recirculation (EGR) and injection timing. Both are limiting the achievable fuel-efficiency, i.e., there exists a NO_x-BSFC trade-off, with the brake specific fuel consumption (BSFC) in [g/kWh].

The industrial standard in Diesel engine control comprises look-up table based feedforward and feedback control. In the literature, different combinations of control variables are suggested, see, e.g., [1], [2], [3], [4], [5]. The availability of in-cylinder pressure sensors (which are not yet standard in trucks) increases the effectiveness of feedback control, as it enables a more direct measurement of the combustion behavior. To be precise, indicated mean effective pressure (IMEP) (related to power) and combustion phasing parameters such as CA_{50} can be measured. Although feedback control improves the robustness of the engine control system in terms of disturbance rejection, the high-level optimization problem of determining the related reference signals is typically addressed by off-line (manual) tuning in an engine test cell. As a result, the obtained performance, in terms of the engine-out NO_x mass flow and fuel-efficiency, remains sensitive to the earlier mentioned real-world disturbances.

Aiming to improve upon this off-line tuning solution, we propose to apply extremum-seeking (ES) for on-line tuning of two of the closed-loop controlled parameter reference signals, which are known to effect the NO_x-BSFC trade-off. ES is an adaptive optimization technique, see, e.g., [6], which aims to optimize a measured cost, with the advantage that very little knowledge about the system dynamics and disturbances is required. The main requirement is that, for steady-state operation, the considered system has a (quasi-)convex mapping from the inputs(s) to be tuned, to the performance output. A variety of ES approaches has been proposed in the context of on-line engine performance optimization. For example [7] or [8] where spark timing is adjusted for spark ignition engines, [9] where the fueling profile of a Diesel engine is adjusted, or [10] where the reference signal for closed-loop controlled CA_{50} is optimized.

In this paper, an on-line measurable cost criterion and constraint outputs are proposed, which connect to the engine control problem of delivering power, using minimal fuel, while satisfying an engine-out NO_x constraint. Minimizing this cost criterion is posed as a constrained two-input (quasi-)convex optimization problem, which effects fuel-path and air-path actuators. An ES controller is applied, in which the scalar constraint handling approach proposed in [11] is extended to multiple constraints. Experimental results

All authors are with the Eindhoven University of Technology, Department of Mechanical Engineering, Control Systems Technology Group, Eindhoven, the Netherlands. Thijs van Keulen is also with DAF Trucks N.V., Eindhoven, the Netherlands. Frank Willems is also with TNO Automotive, Powertrains department, Helmond, the Netherlands {r.v.d.weijst, t.a.c.v.keulen, f.p.t.willems}@tue.nl

are obtained on a Euro-VI heavy-duty Diesel engine, with additional in-cylinder pressure sensors.

This paper is organized as follows. The considered engine, its low-level control system, and the high-level optimization problem are addressed in Section II. The ES method is presented in Section III and the experimental results in Section IV. The conclusions are given in Section V.

II. System description

The high-level goal of Diesel engine control considered in this paper, is to deliver the requested power, with minimal fuel consumption, while satisfying constrained engine-out NO_x emission. First, the engine will be discussed, including the available actuators and sensors, which can be used to satisfy the high-level goal. Subsequently, some properties of an already existing engine control system are given. Eventually, ES is applied to find optimal reference signals for this control system, and therefore it is referred to as the "low-level" control system. This section is concluded by presenting an on-line applicable optimization problem which relates to the mentioned high-level Diesel engine control goal. The engine considered throughout this paper is a state-of-the-art heavy-duty Euro-VI six-cylinder truck engine, with additional in-cylinder pressure sensors and a high resolution crank angle encoder.

A. Engine system

The engine setup is schematically depicted in Fig. 1. In this figure, the engine block, the air-path, the fuel-path, and the dynamo-meter are displayed. The dynamo-meter represents a test cell installation that dissipates the engine power. In the following, the actuators and sensors, which are used for control in this work, are discussed.

1) Actuators: The air-path consists of the turbocharger with variable geometry turbine (VGT) and cooler, and the cooled high-pressure EGR system. Actuation of the air-path is possible using the EGR valve and by adjusting the VGT position. The turbocharger with VGT provides a high turbine efficiency over a wide turbine operating range and control over the exhaust manifold pressure. The EGR system is used to dilute the intake air, which results in a lower combustion temperature, which tempers NO_x formation. However, EGR reduces the fuel efficiency, i.e., there exists a NO_x-BSFC trade-off. One particular reason is that the pressure difference $dp = p_{ex} - p_{in}$ between the exhaust and intake manifold pressures, p_{ex} and p_{in}, respectively, needs to be positive. This pressure difference dp is known as the pumping-loss of the engine, see, e.g., [12], and is used as control output, as proposed in [1].

The fuel-path consists of a common rail system with six injectors, which provides the following control inputs: Start of injection (SOI) and duration of cylinder individual fuel injection pulses. The rail pressure is not used as control input in this work. Fuel injection timing and quantity also influence the NO_x-BSFC trade-off.

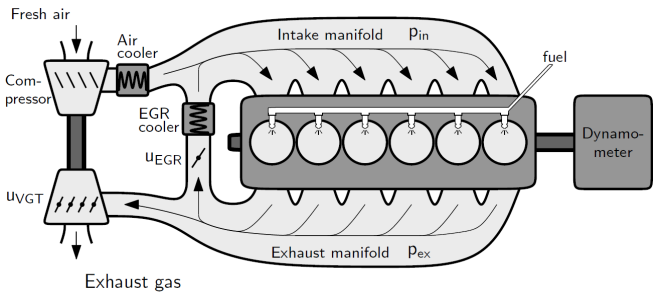

Fig. 1. Schematic outlay of the experimental setup, figure taken from [1].

2) Sensors: Pressure sensors are present to obtain p_{in} and p_{ex} in [kPa]. In addition, a NO_x concentration (in [ppm]) sensor is available, which is known to have some delay. Combined with estimates of the mass air flow and engine power, it provides the engine-out NO_x level in [g/kWh]. The engine is equipped with Kistler 6125 in-cylinder pressure sensors (one in each cylinder) and a high resolution (0.1 degree crank angle) AVL 365 crank angle encoder with an AVL Indimodul. Using the in-cylinder pressure and the crank angle, for each of the six cylinders, the following parameters are obtained: 1) the net IMEP, $IMEP_n$ in [bar], is equal to the indicated work of one complete (four-stroke) cycle and thus relates to power, see [12], and 2) combustion phasing parameter CA_{50} in [°CA], which is the crank angle (CA) relative to top dead centre (TDC), at which half of the total heat is released, see [12]. The implementation is according to [13], see also [14].

B. Low-level engine control system

To summarize, from a control perspective, the engine is a system with input $u \in \mathbb{R}^{14\times 1}$:

$$u = \begin{bmatrix} u_{dur}^\top & u_{SOI}^\top & u_{EGR} & u_{VGT} \end{bmatrix}^\top \tag{1a}$$

with vectors $u_{dur}, u_{SOI} \in \mathbb{R}^{6\times 1}$:

$$u_{dur} = \begin{bmatrix} u_{dur_1} & u_{dur_2} & \cdots & u_{dur_6} \end{bmatrix}^\top \tag{1b}$$

$$u_{SOI} = \begin{bmatrix} u_{SOI_1} & u_{SOI_2} & \cdots & u_{SOI_6} \end{bmatrix}^\top \tag{1c}$$

containing the main pulse injection duration signals in [ms], and SOI in [°CA] relative to TDC, for each of the six cylinders. Signals $u_{EGR}, u_{VGT} \in [0, 100]$ are the EGR valve opening in [%], and the VGT position in [%], respectively. The measured output is $y \in \mathbb{R}^{14\times 1}$:

$$y = \begin{bmatrix} y_{IMEP_n}^\top & y_{CA_{50}}^\top & y_{NO_x} & y_{dp} \end{bmatrix}^\top \tag{2a}$$

with units [bar], [°CA] relative to TDC, [g/kWh], and [kPa], respectively, and vectors $y_{IMEP_n}, y_{CA_{50}} \in \mathbb{R}^{6\times 1}$:

$$y_{IMEP_n} = \begin{bmatrix} y_{IMEP_{n_1}} & y_{IMEP_{n_2}} & \cdots & y_{IMEP_{n_6}} \end{bmatrix}^\top \tag{2b}$$

$$y_{CA_{50}} = \begin{bmatrix} y_{CA_{50_1}} & y_{CA_{50_2}} & \cdots & y_{CA_{50_6}} \end{bmatrix}^\top \tag{2c}$$

containing the cylinder specific measurements.

The low-level engine control system is schematically depicted in Fig. 2. In this figure, $\mathcal{P}$ represents the engine with

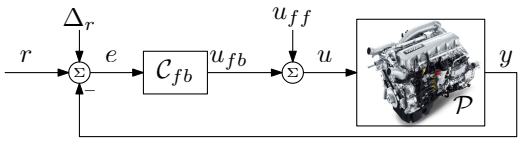

Fig. 2. Low-level control system schematics.

input u in (1) and output y in (2), $\mathcal{C}_{fb}$ is a feedback controller with output $u_{fb} \in \mathbb{R}^{14\times 1}$ and as input the tracking error $e = r + \Delta_r - y$, where $r \in \mathbb{R}^{14\times 1}$ is the reference signal, and

$$\Delta_r = \begin{bmatrix} 0^{1\times 6} & \Delta_{r_{CA_{50}}}^{1\times 6} & 0 & \Delta_{r_{dp}} \end{bmatrix}^\top$$

a delta on the CA_{50} and dp reference signals, where $(\cdot)^{1\times 6}$ indicates a six element row vector. Note that for all six cylinders, the same reference signals $r_{CA_{50}}$ and r_{IMEP_n}, and delta signal $\Delta_{r_{CA_{50}}}$ are used. The reference signal r and feedforward signal $u_{ff} \in \mathbb{R}^{14\times 1}$ are obtained from off-line tuned look-up tables, while Δ_r is the ES input, which will be explained in the remainder of the paper. The low-level level control system offers robust tracking performance of the total reference signal $r + \Delta_r$.

C. High-level optimization problem

Recall the high-level control problem: Delivering power, with minimal fuel consumption, subject to constrained engine-out NO_x emission. Using the low-level control system, the power of the engine can be controlled through r_{IMEP_n}, and the engine-out NO_x level through r_{NO_x}. Note that, in case we set r_{NO_x} equal to the constraint, $e_{NO_x} = r_{NO_x} - y_{NO_x} > 0$ does not violate the constraint. However, $e_{NO_x} > 0$, averaged over time, i.e., its $\mathscr{L}_2$-norm, does not appear in practice, due to the NO_x-BSFC trade-off.

As mentioned in Section II-A, the NO_x-BSFC trade-off can be influenced both via the air-path system, using r_{dp}, as well as the fuel-path system. In the latter case, CA_{50} is the parameter that influences the NO_x-BSFC trade-off. As such, adequate tuning of the reference signals r_{dp} and $r_{CA_{50}}$ is essential to obtain a minimal BSFC. Accordingly, the optimization inputs which are considered in this work are the delta inputs $\Delta_{r_{CA_{50}}}$ and $\Delta_{r_{dp}}$, which adjust the look-up table based reference signals $r_{CA_{50}}$ and r_{dp}.

1) On-line measurable cost function: The actual BSFC cannot be measured, because direct measurements of the fuel mass flow and brake power are not available on the vehicle. Therefore, these values are estimated based on u_{dur} and y_{IMEP_n}. A detailed description of this estimation is beyond the scope of this paper. Summarizing, the estimation is as follows. For a given rail pressure and power demand, i.e. r_{IMEP_n} and engine speed, a minimum injector opening time, which results in the demanded net IMEP, corresponds with the minimum BSFC for that engine power. Hence, by evaluating a cost criteria based on the average injection duration over the six cylinders, fuel consumption optimization is possible without a direct measurement of fuel mass flow. To suppress operating point dependency (i.e. engine speed and load), the proposed cost criterion J, based on injection duration, is normalized. The normalization is achieved by dividing the BSFC estimate by default look-up table based values, as a function of engine speed and r_{IMEP_n}. As a result, we get that $J \approx 1$. In the experimental results in Section IV, it is shown that a decrease in J corresponds to a decreasing BSFC.

The upper left plot in Fig. 3 shows measured steady-state values J_{st} of J, at a grid of $\Delta = \begin{bmatrix} \Delta_{r_{CA_{50}}} & \Delta_{r_{dp}} \end{bmatrix}$, for a typical cruise control engine operating point. To visualize J_{st}, a plane is fitted, which shows that J_{st} is (quasi-)convex, which is beneficial for optimization. We like to stress the relevance of this result in terms of optimization, as the original problem of determining the values of four actuators is reduced to a (quasi-)convex 2D optimization problem. In general, from J_{st} it is seen that a lower dp decreases the BSFC (as expected) and for CA_{50} an optimum exists.

2) Constraints: As a result of the NO_x-BSFC trade-off, minimizing cost J, and the BSFC accordingly, potentially results in pour NO_x tracking. In essence, Δ can be selected such that the low-level control system is unable to achieve a zero steady-state tracking error e. That is, because the low-level control design is based on local linear models of the engine. As such, for example, actuator constraints, or a reduced effectiveness of actuators, are not taken into account.

The issue encountered in practice is a drastic reduction in the effectiveness of the EGR valve. A low dp reduces the effectiveness of the EGR valve, i.e., a higher opening percentage (high value of $u_{fb_{EGR}}$) is required for the same amount of EGR. Correspondingly, NO_x tracking becomes increasingly difficult. To maintain tracking performance, signals $u_{fb_{EGR}}$ and e_{NO_x} are incorporated as constraints, as follows:

$$h_{NO_x} = -e_{NO_x} - \delta_{NO_x} \tag{3a}$$

$$h_{EGR} = u_{fb_{EGR}} - \delta_{EGR} \tag{3b}$$

where $\delta_{NO_x}, \delta_{EGR} \geq 0$ are used for normalization. The constraint h_{NO_x} is required, because a NO_x tracking error is not necessarily due to reduced effectivity of the EGR valve only. On the other hand, opposed to signal $u_{fb_{EGR}}$, the measurement of e_{NO_x} has delay (due to the NO_x concentration sensor). Therefore, it is useful to prevent the EGR valve induced NO_x tracking error, by using the constraint h_{EGR}. The steady-state values $h_{NO_x,st}$ and $h_{EGR,st}$, corresponding to the measurement of J_{st}, are given in Fig. 3. The normalization values are $\begin{bmatrix} \delta_{NO_x} & \delta_{EGR} \end{bmatrix} = \begin{bmatrix} 0.3 & 20 \end{bmatrix}$. Indeed, for low $\Delta_{r_{dp}}$, both constraints are violated.

3) On-line optimization problem: From an optimization point-of-view, the low-level engine control system, including the cost and constraint functions, is one dynamic system, defined as Σ, with input Δ, and outputs J, h_{NO_x}, and h_{EGR}. The optimization problem can be formalized as follows:

$$\min_{\Delta} J \text{ s.t. } h_{NO_x}, h_{EGR} \leq 0, \begin{bmatrix} J & h_{NO_x} & h_{EGR} \end{bmatrix}^\top = \Sigma(\Delta) \tag{4}$$

with h_{NO_x} and h_{EGR} in (3). For the considered operating point, the steady-state version of this optimization problem is given in the lower left plot in Fig. 3, which is constructed using the surfaces in the same figure.

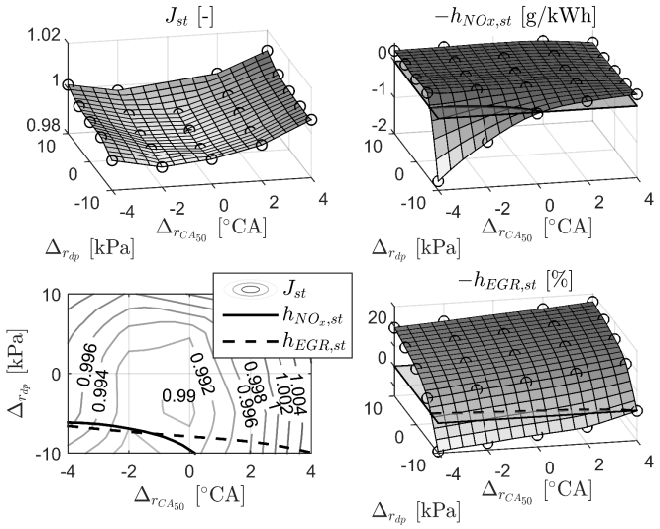

Fig. 3. Measured steady-state values $J_{st}, h_{NOx,st}, h_{EGR,st}$ (black circles) for a grid of $(\Delta_{r_{CA_{50}}}, \Delta_{r_{dp}})$ combinations, for a typical part-load cruise control engine operating point. The fitted surfaces are obtained using a heuristic algorithm. To indicate the constraints, surfaces $h_{NO_x,st}, h_{EGR,st} = 0$ are plotted. The resulting steady-state (constrained) optimization problem is depicted in the lower left plot.

III. Extremum-seeking optimization

In this section, the application of ES to find a solution to the optimization problem (4) is motivated, and the applied ES method is introduced.

A. Extremum-seeking as on-line optimization approach

For a constant operating point, the optimum for the optimization problem (4) derived in Section II-C can be found off-line by manual tuning. In fact, that is how the look-up table based reference signals are obtained. However, due to the influence of production tolerances (e.g. sensor bias), component wearing and fouling, or varying ambient conditions and fuel quality, an off-line determined tuning of the reference signals is not necessarily optimal in practice. Moreover, we do not have an explicit model of system Σ. Therefore, we propose to apply ES, see, e.g., [6]. ES is an adaptive on-line optimization technique which requires very little knowledge about the system Σ. The only requirements are that Σ is stable and possesses a quasi-convex steady-state input output map, see, e.g. [6], for the formal requirements.

B. Extremum-seeking method

The applied ES method employs classical dither-based derivative estimation, see [15], and [16] for the multivariable case. A first-order high-pass filter is applied to the system outputs to remove their DC contribution. A moving average (MA)-filter is applied to suppress harmonic disturbances in the derivative estimates, as proposed in [17], instead of a the usually applied low-pass filter, e.g. in [6]. For the constraint handling, the single constraint approach proposed in [11] is extended such that it is applicable for multiple constraints.

The ES system schematics are depicted in Fig. 4. Inputs $\Delta_{r_{CA50}}$ and $\Delta_{r_{dp}}$ are perturbed by the dither signals

$$d_i(t) = a_{d_i} \cos(\omega_{d_i} t)$$

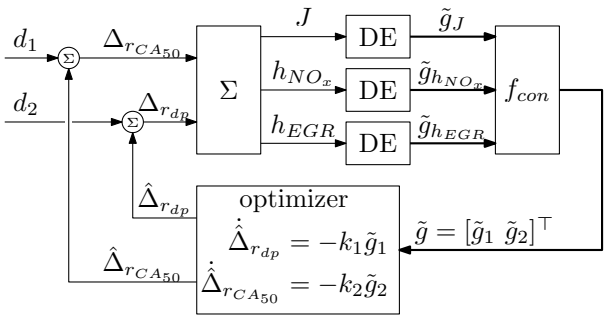

Fig. 4. Extremum-seeking system schematics.

with $a_{d_i}, \omega_{d_i} \in \mathbb{R}_{>0}$, $i = 1, 2$, the dither amplitude and dither frequency, respectively. As proposed in [16], we select $\omega_{d_1} = 2\omega_{d_2}$. The DE blocks estimate the derivatives of cost output J and constraint outputs h_{NO_x}, h_{EGR}, with respect to input $\Delta = \begin{bmatrix}\Delta_{r_{CA50}} & \Delta_{r_{dp}}\end{bmatrix}$. The derivative estimates are denoted by $\tilde{g}_J, \tilde{g}_{h_{NO_x}}, \tilde{g}_{h_{EGR}} \in \mathbb{R}^{2\times 1}$, and obtained, e.g., for h_{EGR}, as follows:

$$\text{DE:} \begin{cases} \dot{x}_{HP}(t) = -\omega_{HP} x_{HP}(t) + \omega_{HP} h_{EGR}(t) \\ y_{HP}(t) = -x_{HP}(t) + h_{EGR}(t) \\ \tilde{g}_{h_{EGR}}(t) = \frac{1}{T_{MA}} \int_{t-T_{MA}}^{t} \begin{bmatrix} 2/a_{d_1} \cos(\omega_{d_1}\tau) y_{HP}(\tau) \\ 2/a_{d_2} \cos(\omega_{d_2}\tau) y_{HP}(\tau) \end{bmatrix} \mathrm{d}\tau \end{cases}$$

where $x_{HP}, y_{HP} \in \mathbb{R}$, $\omega_{HP} \in \mathbb{R}_{>0}$, are the high-pass filter state, output, and frequency, respectively, and $T_{MA} = {}^{(2\pi)}/_{w_{d_2}}$ is the time window of the MA-filter.

For constraint handling, the following scheduling function is used:

$$f_{con}: \ \tilde{g} = \begin{bmatrix} \tilde{g}_J^\top \\ \tilde{g}_{h_{NOx}}^\top \\ \tilde{g}_{h_{EGR}}^\top \end{bmatrix}^\top \begin{bmatrix} (1-\alpha(h_{NO_x}))(1-\alpha(h_{EGR})) \\ \gamma_{NO_x}\alpha(h_{NO_x})(1-\alpha(h_{EGR})) \\ \gamma_{EGR}\alpha(h_{EGR}) \end{bmatrix} \tag{5}$$

with the "smooth switch" function $\alpha : \mathbb{R} \to (0, 1)$, which, for h_{EGR}, is given by:

$$\alpha(h_{EGR}) = \frac{1}{1 + \exp\left(-\frac{1}{\kappa_{EGR} h_{EGR}}\right)}$$

with $\kappa_{EGR} \in \mathbb{R}_{>0}$, $\alpha(h_{NO_x})$ is defined equivalently. Scaling factors $\gamma_{NO_x}, \gamma_{EGR} \in \mathbb{R}_{>0}$ are tuned such that $\gamma_{NO_x}\tilde{g}_{h_{NO_x}}$ and $\gamma_{EGR}\tilde{g}_{h_{EGR}}$ are of similar magnitude as $\tilde{g}_J$. Function f_{con} in (5) yields a combined derivative estimate $\tilde{g}$, which is used in the optimizer indicated in Fig. 4. The optimizer outputs $\hat{\Delta}_{CA_{50}}$ and $\hat{\Delta}_{dp}$ result as indicated in Fig. 4 in the "optimizer" block, with $k_i > 0$, $i = 1, 2$ the optimizer gains. As a result of the scaling factors $\gamma_{EGR}, \gamma_{NO_x}$, the contribution of all derivatives to the combined estimate $\tilde{g}$ is balanced. In [11], an integrator is used for this purpose. Although technically more elegant, the integrator has the disadvantage of windup which is easily avoided by using scaling factors instead.

IV. Engine experiments

The engine setup is already introduced in Section II. In the test setup, the standard ECU is bypassed. To implement the

TABLE I

EXTREMUM-SEEKING PARAMETERS

Parameter	ω_{d_1} [rad/s]	ω_{d_2} [rad/s]	a_{d_1} [°CA]	a_{d_2} [kPa]
Value	0.16π	0.08π	0.4	0.8

T_{MA} [s]	ω_{HP} [rad/s]	δ_{NO_x} [g/kWh]	δ_{EGR} [%]
25	0.072π	0.3	20

γ_{NO_x} [-]	γ_{EGR} [-]	κ_{EGR} [-]	κ_{NO_x} [-]	k_1 [-]	k_2 [-]
0.005	0.001	1	0.01	12	120

low-level and ES controllers, Speedgoat rapid control prototyping hardware is used combined with Matlab/Simulink®. Calculation of y_{IMEP_n} and $y_{CA_{50}}$ is done according to [13], using the FPGA (field-programmable gate array) in the Speedgoat.

A. Extremum-seeking parameters

Tuning of the parameters of an ES controller is not straightforward, as it depends on properties of the system, such as its time-scale and the contribution of disturbances to the measured system outputs. In Table I, an overview of the applied values is given. The tuning is aiming for a high convergence speed, while maintaining a reasonably small region to which the solution converges, similar to the dither amplitude to be precise.

B. Measurement results

Measurements are done with the same engine speed and reference r_{IMEP_n} as is the case for the steady-state results in Fig. 3. To accentuate the ES functionality, non-nominal initial conditions $\Delta_0 = \begin{bmatrix}4 & 5\end{bmatrix}$ and $\Delta_0 = \begin{bmatrix}-2 & 5\end{bmatrix}$ are used. In Fig. 5, plots are given of $\Delta(t)$, $\hat{\Delta}(t)$, and $J(t)$, as a function of time, for the two different Δ_0. Additionally, an MA-filtered version of the cost is given, which is obtained as

$$J_{MA}(t) = \frac{1}{T_{MA}} \int_{t-\frac{1}{2}T_{MA}}^{t+\frac{1}{2}T_{MA}} J(\tau)\mathrm{d}\tau$$

with $T_{MA} = 25$. The MA-filter has a low-pass characteristic.

For both initial conditions, cost $J(t)$ is decreased. Moreover, the solution converges to the same point $\Delta^* \approx [-0.3 \ -6]$, see also Fig. 6 where the $\Delta(t)$ and $\hat{\Delta}(t)$ are plotted in the ES input space. These results roughly coincide with the expectations based on the result in Fig. 3. The differences can be due to day-to-day variations in the system, or to the plane fitting through the measured steady-state points. It is clear that $\Delta^* \neq [0\ 0]$, which indicates that a performance increase compared to the nominal tuning is possible. In the remainder of this section, the measurement with $\Delta_0 = \begin{bmatrix}-2 & 5\end{bmatrix}$ is considered.

In Fig. 7 the values of $h_{EGR}(t)$ and $h_{NO_x}(t)$ are given, which show that $\Delta^* \approx [-0.3\ -6]$ is a constrained optimum. The slight constraint violation is due to the low-level control system dynamics, and measurement delay of $e_{NO_x}(t)$.

Fig. 8 shows the actuator signals $u(t)$, for $u_{dur}(t)$ and $u_{SOI}(t)$, the average over the six cylinders is plotted. A decrease of $u_{dur}(t)$ is visible, which corresponds to a lower fuel consumption. Observe that all four actuators respond to the optimization using only two inputs $\Delta_{r_{CA_{50}}}$ and $\Delta_{r_{dp}}$.

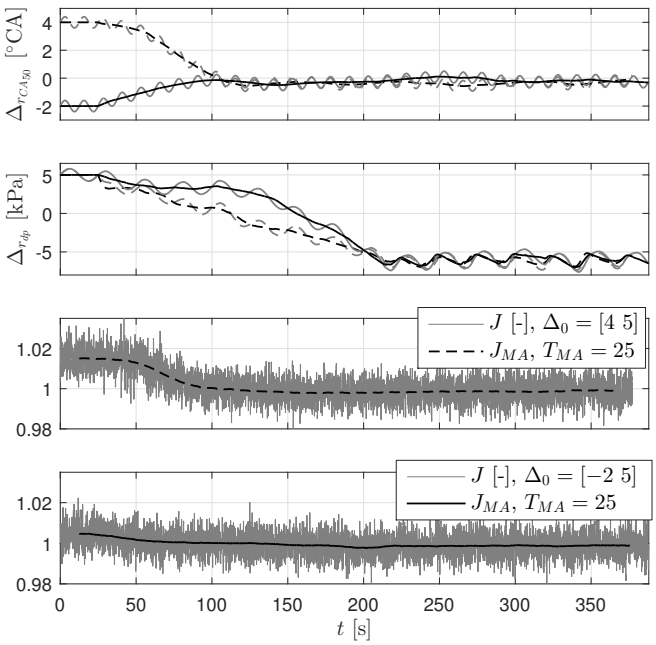

Fig. 5. Inputs $\Delta_{r_{CA_{50}}}$ and $\Delta_{r_{dp}}$, cost J, and MA-filtered cost J_{MA} as a function of time. The dashed and solid lines correspond to $\Delta_0 = [4\ 5]$ and $\Delta_0 = [-2\ 5]$, respectively. The (dashed) black lines in the first two plots are optimizer outputs $\hat{\Delta}_{r_{CA_{50}}}$ and $\hat{\Delta}_{r_{dp}}$, the (dashed) grey lines the total inputs $\Delta_{r_{CA_{50}}} = \hat{\Delta}_{r_{CA_{50}}} + d_1$ and $\Delta_{r_{dp}} = \hat{\Delta}_{r_{dp}} + d_2$.

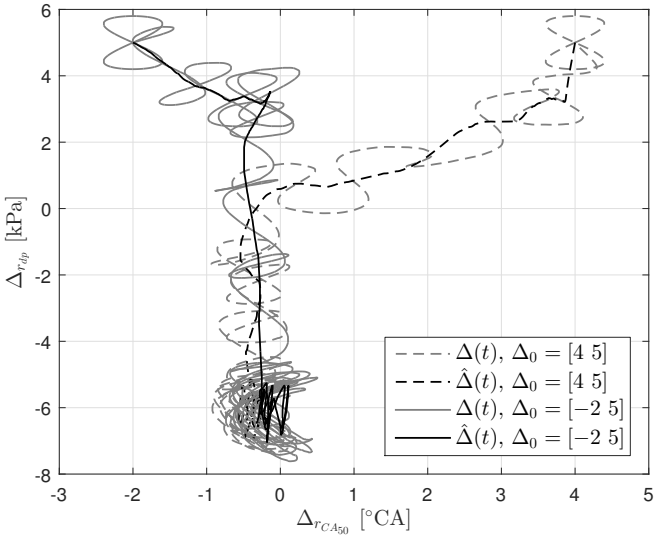

Fig. 6. $(\Delta_{r_{CA_{50}}}, \Delta_{r_{dp}})$ trajectories corresponding to the results in Fig. 5.

Finally, the actual BSFC can be measured in the test setup. The result is given in Fig. 9, which clearly shows a decrease in BSFC over time. This shows that the applied cost function (which also decreases, see Fig. 5) is a good equivalent measure of the BSFC.

V. CONCLUSIONS

A two-input (quasi-)convex optimization problem is proposed, which connects to the Diesel engine control goal of delivering power, using a minimal amount of fuel, subject to constrained engine-out NO_x emission. The two inputs are reference signals of a low-level feedback control system, related to combustion phasing and pumping losses. By using

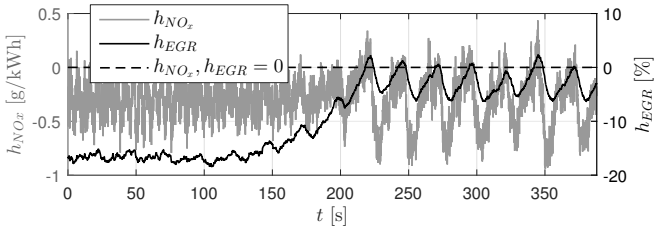

Fig. 7. Constraint outputs h_{EGR} and h_{NO_x} as a function of time, for the measurement with $\Delta_0 = [-2\ 5]$.

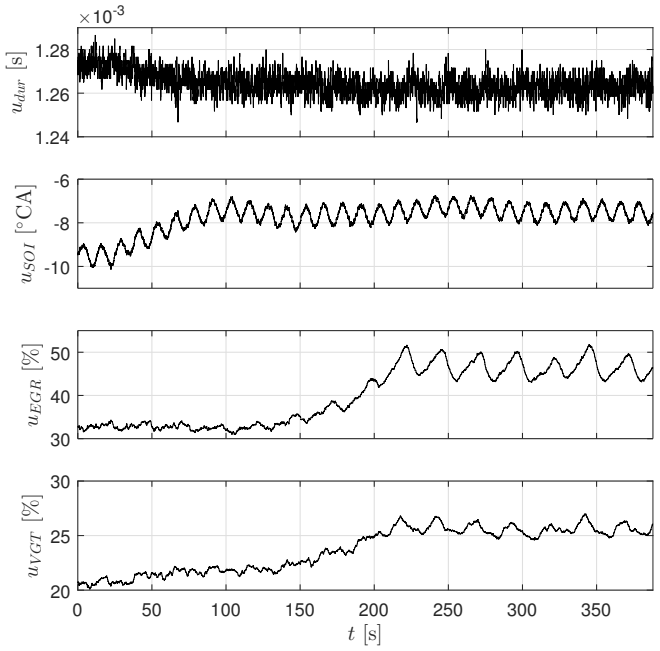

Fig. 8. Actuator positions u for the measurement with $\Delta_0 = [-2\ 5]$. Signal u_{SOI} is defined relative to TDC.

the low-level control system, all air-path *and* fuel-path actuators (four in total) respond to the optimization of only two inputs. The on-line measurable cost output is equivalent to the brake specific fuel consumption (BSFC). A constrained extremum-seeking (ES) approach is applied, which is able to find the (constrained) minimum on-line. By doing so, optimal fuel-efficiency can be achieved, potentially also under real-world disturbances, as no model and disturbances information are required for ES. Experiments are conducted on an advanced setup, based on a Euro-VI heavy-duty truck engine, with additional in-cylinder pressure sensors. The experiments demonstrate the functionality of ES and the equivalence of the proposed cost function to the actual fuel consumption. Future work will include an evaluation of the ES performance on a transient drive cycle, and additional constraints will be included on the hardware.

ACKNOWLEDGMENTS

This research is done in the framework of the TKI research project ES4ACC (Extremum Seeking for Advanced Combustion Control). This project is a collaboration between DAF Trucks and TNO and is partially funded by the Dutch Ministry of Economic Affairs. The authors are specially grateful to Frank Kupper.

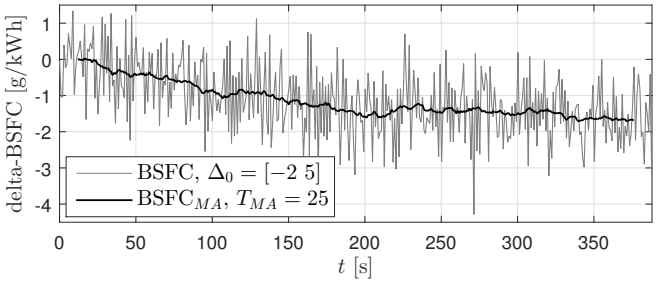

Fig. 9. Normalized BSFC for the measurement with $\Delta_0 = [-2\ 5]$. This result is obtained from measured mass fuel flow and dynamo-meter data.

REFERENCES

[1] C. Criens, F. Willems, T. van Keulen, and M. Steinbuch, "Disturbance rejection in diesel engines for low emissions and high fuel efficiency," *IEEE Transactions on Control Systems Technology*, vol. 23, no. 2, pp. 662–669, 2015.

[2] X. Luo, S. Wang, B. de Jager, and F. Willems, "Cylinder pressure-based combustion control with multi-pulse fuel injection," *IFAC-PapersOnLine*, vol. 48, no. 15, pp. 181–186, 2015.

[3] F. Tschanz, S. Zentner, C. H. Onder, and L. Guzzella, "Cascaded control of combustion and pollutant emissions in diesel engines," *Control Engineering Practice*, vol. 29, pp. 176–186, 2014.

[4] J. Wahlström and L. Eriksson, "Output selection and its implications for MPC of EGR and VGT in diesel engines," *IEEE Transactions on Control Systems Technology*, vol. 21, no. 3, pp. 932–940, 2013.

[5] D. Zhao, C. Liu, R. Stobart, J. Deng, E. Winward, and G. Dong, "An explicit model predictive control framework for turbocharged diesel engines," *IEEE Transactions on Industrial Electronics*, vol. 61, no. 7, pp. 3540–3552, 2014.

[6] Y. Tan, W. H. Moase, C. Manzie, D. Nešić, and I. M. Y. Mareels, "Extremum seeking from 1922 to 2010," in *Proc. of the Chinese Control Conference*, 2010, pp. 14–26.

[7] A. Mohammadi, C. Manzie, and D. Nešić, "Online optimization of spark advance in alternative fueled engines using extremum seeking control," *Control Engineering Practice*, vol. 29, pp. 201–211, 2014.

[8] E. Hellström, D. Lee, L. Jiang, A. G. Stefanopoulou, and H. Yilmaz, "On-board calibration of spark timing by extremum seeking for flex-fuel engines," *IEEE Transactions on Control Systems Technology*, vol. 21, no. 6, pp. 2273–2279, 2013.

[9] M. Großbichler, R. Schmied, P. Polterauer, H. Waschl, and L. del Re, "A robusrobust based extremum seeking for engine optimization," in *Proc. of the American Control Conference*, 2016, pp. 3280–3285.

[10] M. Lewander, A. Widd, B. Johansson, and P. Tunestål, "Steady state fuel consumption optimization through feedback control of estimated cylinder individual efficiency," in *Proc. of the American Control Conference*. IEEE, 2012, pp. 4210–4214.

[11] M. Ramos, C. Manzie, and R. Shekhar, "Online optimisation of fuel consumption subject to nox constraints," in *Preprints of the 20th IFAC World Congress, Toulouse, France, 9-14 July 2017*, 2017, pp. 9231–9236.

[12] J. B. Heywood, *Internal Combustion Engine Fundamentals*. McGraw-Hill, 1988.

[13] C. Wilhelmsson, P. Tunestål, and B. Johansson, "Model based engine control using asics: A virtual heat release sensor," *Les Rencontres Scientifiques de l'IFP:" New Trends in Engine Control, Simulation and Modelling"*, 2006.

[14] F. Willems, E. Doosje, F. Engels, and X. Seykens, "Cylinder pressure-based control in heavy-duty EGR diesel engines using a virtual heat release and emission sensor," 2010, pp. 2010–01–0564–1/12.

[15] D. Nešić, Y. Tan, W. H. Moase, and C. Manzie, "A unifying approach to extremum seeking: Adaptive schemes based on estimation of derivatives," in *49th IEEE Conference on Decision and Control*, 2010, pp. 4625–4630.

[16] R. van der Weijst, T. van Keulen, and F. Willems, "A generalized framework for perturbation-based derivative estimation in multivariable extremum-seeking," vol. 50, no. 1, 2017, pp. 3148 – 3153, 20th IFAC World Congress.

[17] M. Haring, N. Van De Wouw, and D. Nešić, "Extremum-seeking control for nonlinear systems with periodic steady-state outputs," *Automatica*, vol. 49, no. 6, pp. 1883–1891, 2013.